JOURNAL OF Materials CHEMISTRY

Porous hydroxyapatite–dodecylphosphate composite film on titania–titanium substrate

Ivana Soten and Geoffrey A. Ozin*

Materials Chemistry Research Group, Lash Miller Chemical Laboratories, 80 St. George Street, University of Toronto, Toronto, Ontario, Canada M5S 3H6.
E-mail: gozin@alchemy.chem.utoronto.ca

Received 3rd August 1998, Accepted 8th December 1998

Synthetic analogues of bone are being actively pursued as materials for biomedical applications in the field of bone replacement, augmentation and repair. Numerous stringent criteria have to be met for a biomaterial to be considered as an acceptable bone implant, including the ability to integrate into bone and not cause any deleterious side effects. In this article we describe a materials chemistry approach to synthesizing a new type of bone implant material. The strategy involves the spontaneous growth, under aqueous physiological pH conditions, of an oriented hydroxyapatite film with micron dimension porosity, on the surface of a layer of TiO_2 that has been sputter deposited on Ti metal. This procedure creates desirable co-crystallized phases of hydroxyapatite (OHAp) and octacalcium phosphate (OCP) with preferred orientation respectively along the [00l] and [101] directions. Subsequently, a calcium dodecylphosphate mesolamellar phase has been grown within these oriented porous films to create a multilayered chemical composite CaDDP-OHAp-TiO_2-Ti in which the CaDDP phase is stereochemically and charge matched with the OHAp.

Introduction

Bone consists of roughly 70% hydroxyapatite mineral embedded in an organic matrix consisting largely of collagen. Needle-like or plate-like morphologies of hydroxyapatite crystallize at regular intervals along the collagen fibers with their long *c*-axes oriented parallel to the fibrils.[1] Moreover, hydroxyapatite crystals are found around the fibrils, randomly seeded in the collagen matrix and not intimately interacting with the collagen. The presence of HPO_4^{2-} groups in bone apatites has suggested octacalcium phosphate (OCP) to be a precursor to hydroxyapatite (OHAp) formation in bone. In fact, spontaneous hydrolysis of OCP has been observed to result in the formation of non-stoichiometric OHAp (ns-OHAp).[2–4] Non-stoichiometric apatite can exist in three forms: OCP-OHAp intergrowths, imperfectly hydrolyzed OCP, and OHAp formed directly without a precursor.[3] Since the third possibility is not probable under physiological conditions, the presence of non-stoichiometric apatites in the early stage of bone formation as well as in some mature ones has suggested OCP as a precursor. OCP serves to establish the final morphology, composition, solubility, and interfacial energy of apatitic materials, as well as controlling the nucleation and growth of OHAp.[3] These result from the fact that OCP and OHAp have similar crystal structures and are able to epitaxially grow together. As a consequence of this relationship, a prime consideration in the preparation and performance of a bone implant material is the selection of a surface that is able to induce nucleation of OCP.

Different approaches to the preparation of possible bone implant materials have been studied extensively.[5–10] In certain studies metals or metal alloys are used directly as implants,[11] or these are coated with bioactive materials, such as hydroxyapatite.[12,13] Good biocompatibility of certain metals, for example titanium, is thought to occur as a result of spontaneous formation of a thin titanium oxide layer on the surface. This in turn is responsible for the low corrosion rate. Although metals or metal alloys meet biomechanical requirements of implants and some meet biocompatibility requirements, some *in vitro* experiments suggested that coating them with calcium phosphate phases may facilitate healing of the bone and tissue around the implant material. It should be noted that the mechanism of how the surface coatings influence the bone growth at the bone-implant interface are still subject to debate. Different methods for preparing surface overlayers for implants have been explored such as dip coating, chemical vapor deposition, electrophoretic deposition, and plasma spray-coating being the most widely used. However, coating of internal cavities of complex-shaped implant materials is not feasible and the stoichiometry of the coated phase is hard to control.[6] Furthermore, porous bioactive coatings exhibit better bone ingrowth properties[9,14] and the plasma spray-coating technique is able to produce only dense, ceramic materials. Lack of strong adhesion between coatings and metal substrates is an additional problem.

One of the most promising approaches to bone implant materials is the use of composite organic–inorganic materials since in principle they can be designed to be compositional, structural and functional analogues of bone. Different combinations of materials have been used with one of the most well known examples being polymer–hydroxyapatite composites. Moreover, because organic and polymeric structures are used as a targeted drug delivery system, it is easy to imagine how composite inorganic-organic bone analogue materials could facilitate bone repair and overcome infection. With this goal in mind it has been suggested that materials of choice could be a composite of a calcium phosphate-based mesophase and hydroxyapatite.[5,15]

In this study we report details of the spontaneous growth of a porous oriented hydroxyapatite film on a sputter deposited TiO_2 layer on a Ti surface. The results indicate strong adhesion and rapid growth up to 16 μm thick film of calcium phosphate on the TiO_2 surface within hours, rendering them as a viable option for bone implant materials. Both oriented octacalcium phosphate and hydroxyapatite phases are found to co-crystallize in the film by an epitaxial growth process. It is found that OCP acts as a precursor nucleation phase at the TiO_2 surface, that hydrolyzes to hydroxyapatite and continues to grow epitaxially. Subsequently, the calcium dodecylphosphate (CaDDP) lamellar phase was assembled and deposited in a charge and geometry matched fashion on the surface of porous oriented hydroxyapatite on TiO_2. This creates an inorganic–organic composite film architecture distinct from a

physical mixture of the two components. A multi-analytical approach is employed to follow the nucleation and growth process and characterize the composition and structure of the calcium phosphate composite film on the titania–titanium substrate.

Experimental

Preparation of calcium phosphate on the TiO_2 surface

Titanium foil was cut to a size of 10×8 mm, washed with ethanol and air dried. The resulting clean substrates were sputter coated with titanium oxide using a Ti target in a mixed oxygen–argon atmosphere. For optimum results, sputtering was performed for 6 h and the thickness of the oxide layer produced was found to be *ca.* 900 Å using a quartz crystal microbalance.

The substrates prepared were placed on the bottom of polypropylene bottles in 100 ml of solution with the following concentrations: 1.6×10^{-4} M $CaCl_2$ and 7.6×10^{-3} M K_2HPO_4. The pH of the resulting solution was close to physiological, *i.e.* pH of 7.4, the solutions were completely clear and no precipitation was observed throughout the duration period of the experiment. The solutions were aged at 37 °C for periods of 7–120 h. After different times, the substrates were removed from the solutions, carefully washed with deionized water to remove any non-adsorbed electrolytes, and dried under ambient conditions. The pH of the solutions after the substrates were removed was measured to be in the range 7.0–7.2. Control experiments with different initial pH were performed (see below).

Preparation of CaDDP/CaP composite material on the surface of TiO_2

Mono-*n*-dodecylphosphate was transformed to the water soluble form, potassium dodecylphosphate (K_2DDP) with a solution of potassium hydroxide in a ratio of KOH : DDP = 2 : 1. The concentration of K_2DDP in water was 0.1%. The TiO_2 substrate with hydroxyapatite grown on it was placed vertically in a beaker containing K_2DDP by clamping it with custom-made tweezers. The substrate was kept in the solution for 30 min after which time one molar equivalent of a 0.01 M solution of $CaCl_2$ was slowly added to form the CaDDP lamellar phase. The rate of addition of $CaCl_2$ solution was 1ml/15 min. The solution was stirred at a constant rate at 50 °C for 24 h. Following the CaDDP deposition, the substrates were rinsed with copious amounts of water and air dried.

Instrumentation

Coating of the titanium substrate was performed using a Perkin Elmer 2400 sputtering apparatus. Titanium dioxide was produced using a titanium target and mixed argon–oxygen atmosphere. Sputtering was performed for different periods of time at 1000 V dc, using 12 mTorr pressure of 6 sccm argon and 6 sccm oxygen. By adjusting the sputtering conditions, the deposited film could be arranged to be crystalline rutile and/or anatase or amorphous titania. Sputtering conditions were varied in order to produce titania phases anatase, rutile and a mixture of the two on the titanium substrate. These phases were characterized by PXRD. It turns out that the nature of the titania film did not have a dramatic effect on the structure, orientation or composition of the hydroxyapatite overlayers (see below).

Powder X-ray diffraction (PXRD) data were obtained on a Siemens D5000 diffractometer using Ni filtered Cu-Kα radiation ($\lambda = 1.54178$ Å) and a Kevex solid detector. The step size was 0.04° and the step time 1.5 s for the scan range 2θ 1.2–40°. Scanning electron microscopy (SEM) images were obtained on a Hitachi S-570 electron microscope using an accelerating voltage of 15 kV. Transmission electron microscopy TEM images were obtained on a JEOL 2010F field-emission electron microscope FETEM operating at 200 kV by Dr. Aleksandra Perovic. The minimum probe diameter was *ca.* 0.4 nm. Analytical techniques employed were high resolution phase contrast imaging and selected area electron diffraction SAED. The samples were embedded in a TAAB epoxy matrix, cured at 60 °C for 24 h and sectioned using an ion-beam milling technique. The thin sections were then mounted on either carbon coated, plastic coated or 400 mesh size 3.05 mm copper support grids. TEM images were obtained on a Phillips 430 microscope operating at 100 kV by Dr Neil Coombs. The sample was scraped from the Ti/TiO_2 substrate with a razor blade, embedded in a TAAB epoxy matrix and sectioned using a diamond knife. Thin sections were mounted on 400 mesh size 3.05 mm copper support grids. X-Ray photoelectron spectroscopy (XPS) was performed using a Laybold MAX 200 XPS apparatus. A non-monochromatized Mg-Kα X-ray source was used at 15 kV and 20 mA. All the spectra were collected under a vacuum of $< 1 \times 10^{-8}$ Torr. Binding energies are listed in Table 1. Satellite line subtraction was performed as well as correction for charging effects by calibrating the position of the carbon 1s peak at 285 eV. Thickness measurements were performed on a WYKO RST surface roughness tester. The principle of this optical profilometric technique is based upon constructive interference between light that is reflected from the surface and a reference beam, and has a quoted vertical resolution of *ca.* 1 nm. Vertical scanning interference mode was used with a tungsten–halogen lamp as the light source and solid-state CCD detector. Magnifications of 10 and 20 × were used which corresponds to 422×468 μm and 211×234 μm, respectively. One part of the Ti/TiO_2 substrate was masked with a sticky tape during the crystal growth and removed before the measurement. The thickness of the calcium phosphate film was measured with respect to the non-covered area and the average peak to valley height value was used as thickness values. Other parameters such as roughness, average roughness and maximum peak to valley height were also obtained by this technique. NMR data were collected on 400 MHz Bruker Avance DSX spectrometer. Samples that were grown on the Ti/TiO_2 substrates were scraped off prior to packing inside the ZrO_2 spinners. The standard for calibration of ^{31}P data was H_3PO_4. For CP MAS NMR the samples were spun at 6 KHz using a recycle delay of 10 s, 90° pulse width of 3.5–4.5 ms and a contact time of 1 ms.

FTIR microscopy spectra were collected on Spectra-Tech IR-Plan laboratory microscope equipped with targeting and redundant aperturing. The former confines the IR radiation to a smaller area, greatly reducing scatter from the matrix surrounding the area of interest while the latter further eliminates scatter from the matrix. For all the samples, diffuse reflectance spectroscopy was used with a 15 mm working distance and a 100 μm pinhole which determined the area that was analyzed. Spectra were recorded from various parts of the substrate.

Results and discussion

Hydroxyapatite grown on a TiO_2–Ti substrate

Fig. 1 displays SEM images of samples obtained after 7, 22, 30 and 48 h of aging. During the early stages (7 h) small 1 μm sized aggregates are observed, which upon increased aging time serve as nucleation sites for subsequent growth of larger plate-like crystals. The crystal plates appear oriented perpendicular to the substrate and upon further aging increase in size and coalesce to form 'rose-like' structures. The entire substrate surface is uniformly covered within *ca.* 30 h. In addition, the coating does not have the texture of a dense calcium phosphate film but instead displays a porous structure

Table 1 XPS data for Ti-TiO_2-OHAp samples obtained after different growth times

Growth time/h	Atomic concentrations[a] (%)				Ca/P ratio	E_B[b]/eV			
	Ca	P	O	Ti		Ca	P	O	Ti
1	1.9	1.7	44.8	12.1	1.1	347.1	133.2	530.0, 531.4, 532.8	458.7
2	1.5	1.5	43.8	9.8	1.0	347.1	133.3	529.8, 531.1, 532.6	458.5
3	1.7	1.6	44.9	11.6	1.1	347.3	133.3	530.0, 531.3, 532.5	458.7
4	3.7	3.1	45.6	11.2	1.1	347.3	133.3	529.8, 531.1, 532.5	458.5
5	3.8	3.1	44.5	8.8	1.2	347.4	133.3	529.9, 531.4, 532.6	458.6
7	7.8	6.1	49.3	6.9	1.3	347.3	133.1	529.8, 531.2, 532.8	458.4
22	13.8	10.0	50.0	2.0	1.3	347.3	133.1	529.9, 531.1, 532.7	455.9
30	15.9	12.1	49.3	0.5	1.3	347.3	133.3	531.3, 533.1	—
48	14.3	11.7	46.0	0	1.2	347.4	133.3	531.3, 533.1	—
72	13.7	11.7	45.2	0	1.2	347.3	133.3	531.3, 533.2	—

[a]Estimated error = 0.1%. [b]Estimated error 0.2 eV.

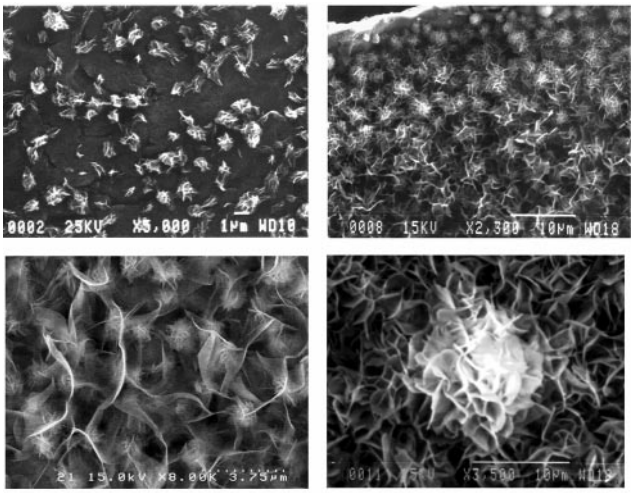

Fig. 1 SEM micrographs of hydroxyapatite grown on TiO_2 after 7 (top left), 22 (bottom left), 30 (top right) and 48 h (bottom right) growth time. Note the micron dimension porosity of the final film.

with an average pore size of *ca.* 1–4 μm. It should be noted that OCP crystals and not OHAp are commonly associated with a plate 'rose-like' morphology.[2,3] As remarked above, a porous apatitic structure is advantageous in certain bone implant situations. Cross-sectional TEM imaging studies of these films revealed direct contact of the calcium phosphate crystals with the TiO_2 substrate. The integrity of the resulting films, irrespective of the aging time, was maintained even after extensive washing and has prolonged shelf-life. It required the application of considerable force with a razor blade to even remove a small part of the film indicating an impressive strength of adhesion.

In order to identify the phases formed, PXRD studies were performed on the obtained film samples. The results are displayed in Fig. 2. The PXRD pattern in Fig. 2(a) is of the film on the TiO_2 surface after 72 h aging time. This pattern was observed after 30 h and before this period nothing was discernible as the film was insufficiently thick to observe a diffraction pattern. The peaks are indexed to a hydroxyapatite phase and the high intensity of the 002 reflection indicates preferential orientation of the crystals along the (001) plane.[16] If the sample contained OCP oriented with the (001) plane parallel to the surface then the most intense reflection from the (100) set of planes would not be seen. When the sample was scraped from the surface and ground, a peak at 18.98 Å was observed that is assigned to the 100 reflection of OCP, Fig. 2(b). Aside from this low angle peak, the remaining peaks are indexable to a hydroxyapatite and not an octacalcium phosphate phase. From these results it can be concluded that the material which forms on the TiO_2 surface consists of an

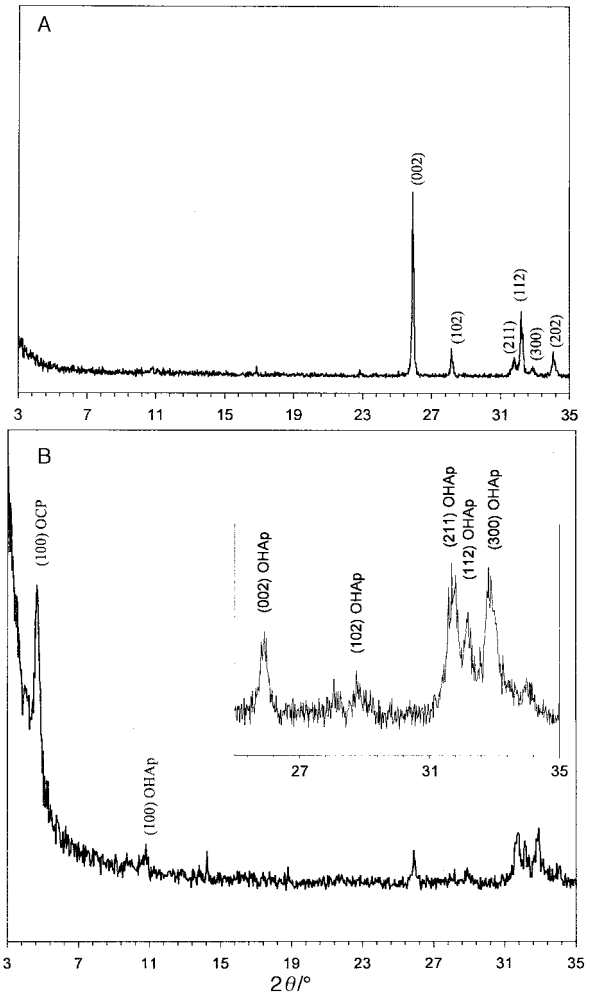

Fig. 2 PXRD patterns of (a) film on the TiO_2 surface after 72 h growth time (all peaks correspond to OHAp phase); (b) film scraped from the substrate and ground to a randomly oriented powder. The film is comprised of oriented OHAp and OCP, the latter being a minor phase.

intergrown mixture of OCP and OHAp, the latter being the predominant phase and the former a minor one.

The thickness of the calcium phosphate films grown on the TiO_2 surface as a function of aging time is shown in Fig. 3. It can be seen that during the first 22 h, the surface is not completely covered and the growth rate is determined primarily by the slow nucleation step. Upon increasing the aging time, the rate appears to increase and suggests that the growth rate is no longer controlled by the nucleation rate on the substrate but is instead dependent upon the production of the earlier formed hydroxyapatite crystals. Films with a thickness up to

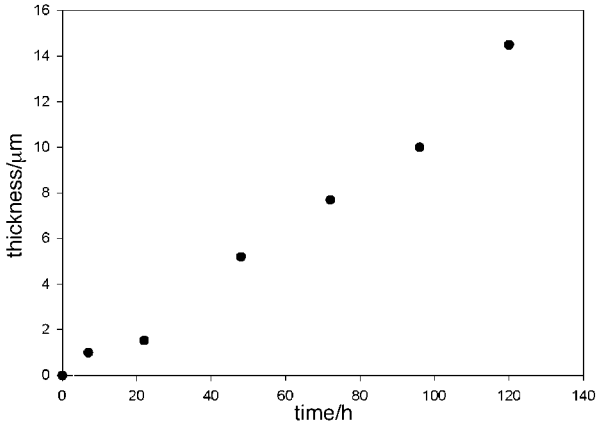

Fig. 3 Thickness of calcium phosphate films as a function of growth time obtained by surface profilometry; error bars too small to be seen.

16 μm were obtained after 5 days but given more time they grow thicker.

In order to further elucidate the role of OCP and OHAp in the formation of these films, time dependent FTIR microscopy studies were performed. It should be noted that the FTIR spectra of hydroxyapatite have two ranges of interest: ν_4 (680–710 cm^{-1})[17] and ν_3 (1000–1200 cm^{-1}).[18] Slight changes in the phosphate ion environment are readily observed by the splitting of the degeneracy of the ν_3 vibration.[18,19] This region can be further sub-divided into two components: 1000–1085 and 1085–1200 cm^{-1} where the lower component is generally more intense. In stoichiometric apatites (s-OHAp) vibrations arise from symmetric ν_1 and antisymmetric ν_3 P–O stretching modes in the region 950–1200 cm^{-1} and ν_4 antisymmetric P–O bending modes at 680–710 cm^{-1}. In non-stoichiometric apatites (ns-OHAp), the presence of HPO_4^{2-} groups and vacancies distort the pattern of P–O stretching modes. These give rise to additional bands which have been extensively assigned and tabulated in the literature.[2,16,18,20] In addition, the OCP phase gives rise to IR spectra that are quite distinct from s-OHAp and ns-OHAp.[21] The presence of bands at 830, 910 and 1200 cm^{-1} are diagnostic of the OCP phase.

Fig. 4 displays the FTIR microscopy spectra of the films grown on titania with all band positions and assignments listed in Table 2. It can be seen that after 7 h, characteristic bands of HPO_4^{2-} ions are present in the sample. This signals the presence of a calcium deficient ns-OHAp phase. In addition, characteristic peaks from OCP are also present, specifically at 867, 917 and 1200 cm^{-1}. These bands were however, only observed after 48 h of aging time. It should be noted that under the synthesis conditions used to grow these films, OCP is commonly believed to be a precursor to OHAp. The observance of OCP only after 48 h implies that at earlier times in the growth process, the amount of OCP present was insufficient to be detected by this FTIR microscopy technique. It may be suggested that the absence of OCP is likely due to its hydrolysis to OHAp. As was mentioned for Fig. 3, initially the growth rate of the film is slow. During this induction time OCP is able to convert to OHAp and hence may account for it not being detected by FTIR. However, once the growth rate increases (after 30 h), the rate of hydrolysis of OCP to OHAp is comparably slower and there exists the likelihood of forming an intergrown OCP/OHAp mixture as recognized by the presence and subsequent increase of OCP P–O vibrational modes in the FTIR spectrum. This proposal receives support from selected area electron diffraction studies of the films as described below.

Electron diffraction (ED) patterns obtained are displayed in Fig. 5. These were obtained using a small aperture size in order to ensure that the cross sectional area examined belonged to a selected small region of one crystal and was *ca.* 0.1 μm in

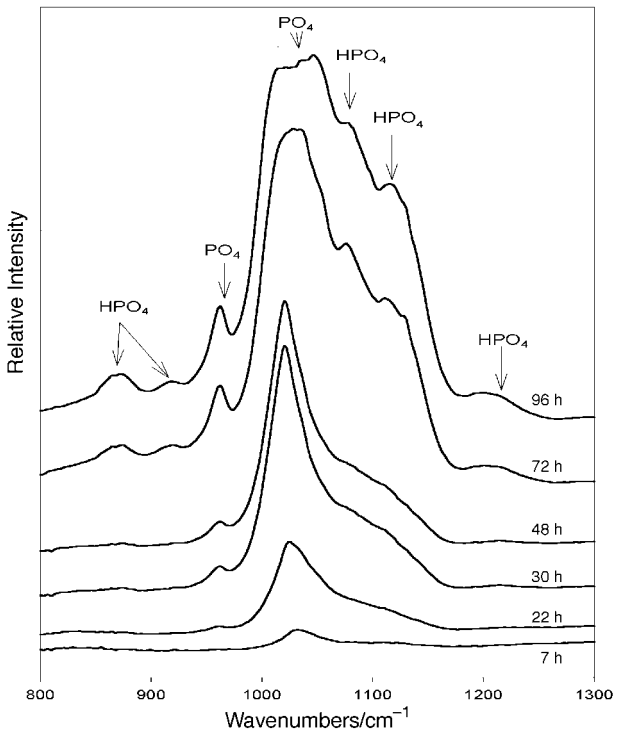

Fig. 4 FTIR microscopy spectra of calcium phosphate films on the TiO_2 substrate after different growth times. Note that the HPO_4^{2-} bands grow in intensity with increased growth time.

Table 2 FTIR band positions (cm^{-1}) and assignments of hydroxyapatite and octacalcium phosphate phases of the films after different growth times[a]

Time/h							
7	22	30	48	72	96	120	Assignment
				872	873	867	ν $HPO_4(5)$ P–(OH) stretch
				917	919	918	ν $HPO_4(6)$ P–(OH) stretch
960	962	961	962	960	961	960	ν_1 PO_4
1007	1000	998	996	1000	997	998	ν_1 HPO_4
1024	1019	1020	1016	1017	1021	1017	ν_3 PO_4
1033	1033	1035	1036	1035	1035	1036	ν_3 PO_4
1056	1052	1055	1056	1054	1058	1055	ν_3 PO_4
1077	1075	1076	1078	1075	1078	1075	ν_3 HPO_4
1096	1097	1096	1093	1096	1093	1093	ν_3 HPO_4
1110	1112	1109	1105	1112	1109	1110	ν_3 $HPO_4(5)$
1122	1119	1117	1120	1124	1123	1123	ν_3 $HPO_4(6)$
1146	1140	1140	1130	1138	1136	1136	ν_3 HPO_4
			1210	1205	1200	1206	δ $HPO_4(5)$ OH in plane bend

[a] $HPO_4(5)$ groups are located in the hydrated layers and $HPO_4(6)$ are located in the junction of the apatitic and hydrated layers in the OCP phase.

size. This was also done to prevent contributions from streak and ring distortions of the ED patterns arising from the expected mosaicity of the samples. The patterns obtained were indexed to the hexagonal lattice of hydroxyapatite viewed along the <1210> zone, Fig. 5(a). Electron diffraction of the triclinic OCP lattice down the <010> zone was also observed, Fig. 5(b). It should be noted that on scanning numerous areas of the films, the majority of the patterns obtained belonged to the OHAp phase and the minority were for the OCP phase. The zones observed confirmed the presence of preferred orientation of both phases. This is because the electron beam was parallel to the substrate which suggested that the zones observed contained only the information regarding planes that were parallel to the substrate. Therefore, the (001) and (101)

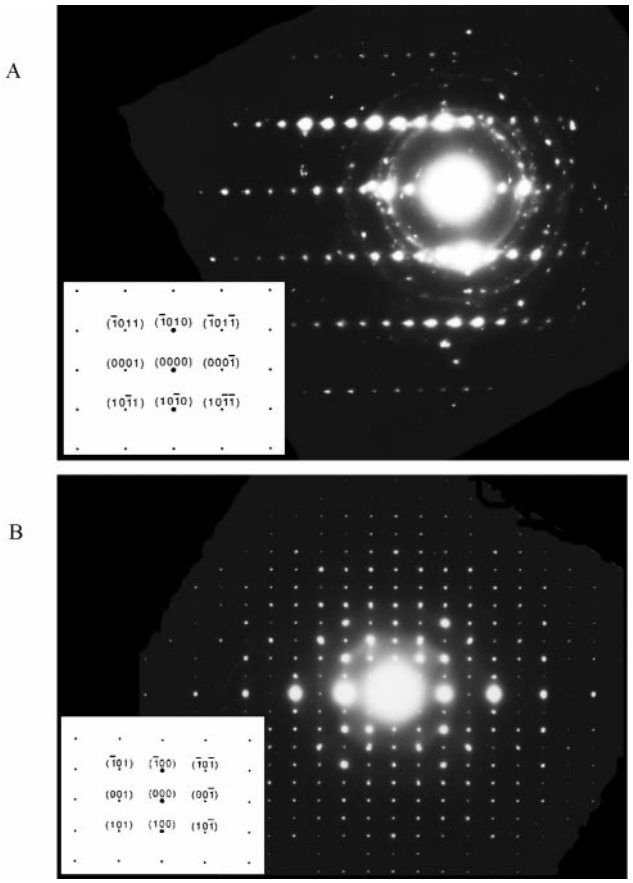

Fig. 5 Selected area electron diffraction (SAED) of (a) <1210> zone of hydroxyapatite; (b) <010> zone of octacalcium phosphate (inserts show indexed simulated ED patterns of appropriate zones).

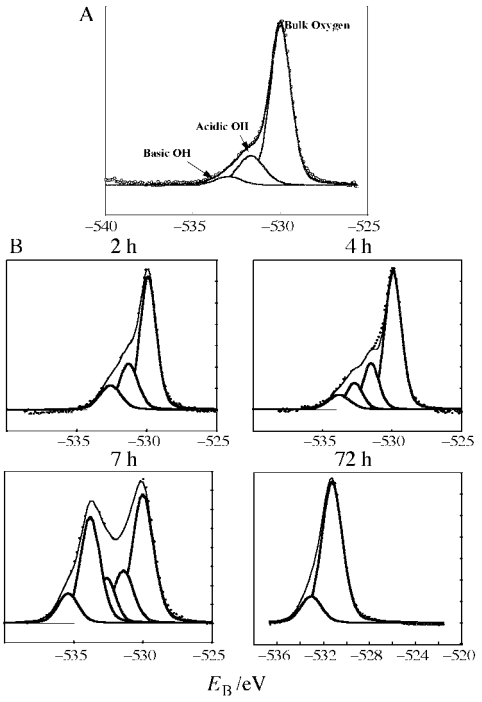

Fig. 6 O 1s XPS spectra of (a) TiO_2 surface before immersion in calcium phosphate solution; (b) TiO_2 surface at different growth times after immersion in calcium phosphate solution. The results indicate that calcium and phosphate ions respectively anchor to the Brønsted acid and base sites of the titania.

planes for both phases are parallel to the substrate as they are contained within the zones observed. In addition, the OCP electron diffraction patterns were obtained from regions mostly on the edges and top parts of the hydroxyapatite crystals that were the furthest away from the substrate. This further confirmed the FTIR results that the presence of OCP could only be detected after prolonged aging times.

In order to further determine the interaction between the substrate and the calcium phosphate film formed, XPS studies were performed. The oxygen 1s binding energies spectra are shown in Fig. 6. Also, Table 1 lists the atomic percentages and binding energies of the representative elements observed by XPS. The presence of both calcium and phosphorus was confirmed after only 1 h of deposition time with a ratio of Ca/P of *ca.* unity. This can be explained by the fact that at pH = 7.5, the surface of TiO_2 is known to be hydroxylated and Brønsted acid and base hydroxy sites exist at the surface that can act as nucleating/anchoring centers for calcium and phosphate groups. Such a TiO_2 surface has two- and three-coordinate bridging oxygens and five- and six-coordinate titanium.[22] After exposure to water the surface becomes hydroxylated and two different types of OH groups exist on the surface. One is denoted as acidic, the other basic and these are distinguishable by means of XPS as seen in Fig. 6(a) and described in the published literature.[22,23]

Quantitative XPS studies of the nucleation and growth of these films shows that the atomic concentrations of Ca and P do not change in the first 3 h after which they increase slightly with time. The first 3 h can therefore be considered as an induction–nucleation period, followed for the next 30 h by a nucleation–crystal growth period. Note the disappearance of the titanium signal from the substrate indicating complete coverage. After the first 3 h of growth, the ratio of bulk to surface oxygen signal decreases due to the higher degree of hydration of the TiO_2 surface in the aqueous solution and also because of the presence of phosphate ions. Also after this time differential charging of the substrate and film is apparent. There are two sets of signals from equivalent atoms, one from atoms close to the TiO_2 surface that are not charging and the other from atoms further from the TiO_2 surface that are charging. Signals from oxygen in hydroxyapatite overlap with oxygens from the substrate surface. This charging is therefore indicative of the formation of the calcium phosphate. After 48 h of aging time the surface is completely covered and the XPS signal originates solely from the calcium phosphate. Two peaks are observed with binding energies at 531 and 533 eV. The former is the reported value for oxygen associated with the phosphate group in hydroxyapatite and the latter is characteristic of oxygen in the HPO_4^{2-} group and intercrystalline water.[4,24–26] The same charging effect is seen with the calcium and phosphorus signals. The binding energies of Ca 2p and P 1s at 347.3 and 133.3 eV respectively, are in agreement with the values reported for hydroxyapatite.[4,24–26] The ratio of Ca/P oscillates around the value of 1.3 in samples obtained after the nucleation period was over (longer than 3 h) which points to the presence of a ns-OHAp. This is in agreement with the FTIR microscopy results presented above.

In order to further prove that OCP is a prerequisite for the growth of the obtained OHAp phase, control experiments were performed. When the conditions of the synthesis were changed in a way so as to favor OHAp nucleation rather then OCP such as, high pH, high temperature and the presence of fluoride, no crystal growth was observed even after five days. XPS spectra showed an interesting result whereby the presence of calcium and phosphorous was in fact observed, albeit in a very small amount and in a 1 : 1 ratio. These values however, did not change upon increased aging time. Conversely, when a lower pH (<7) was used which would allow for nucleation of OCP, again film formation was not observed. XPS spectra showed the absence of calcium or phosphorous on the substrate surface.

Taken together, these results can be explained by the fact that in the case of favorable OHAp nucleation, the surface of the substrate has both acidic and basic activating-anchoring sites to accommodate both calcium and phosphate species but the inability of OCP to nucleate prevented any crystal growth. On the other hand, with a lower pH, OCP could nucleate but the surface was protonated which prevented calcium and phosphate ions from simultaneously binding to the surface. It was concluded therefore that the presence of OCP as a precursor phase and the optimal pH of the initial solution were both pivotal factors that have to be controlled for the successful growth of porous, oriented and thick hydroxyapatite crystalline films on the surface of TiO_2 on Ti. As was mentioned in the Experimental section, changing the titania phase on the substrate did not influence growth of the films in any way. From the PXRD patterns of rutile, anatase and mixtures of the two obtained on the titanium substrate, it was concluded that the sputtering technique produced non-oriented titania with small particle size. Therefore, in the case of all the phases present, some of the particles had an orientation which exposed planes with both acidic and basic hydroxy groups on their surface. Since the presence of both of these groups are responsible for the formation of hydroxyapatite films, a change of the titania phases did not influence the growth of the films.

CaDDP–CaP composite on TiO_2 surface

Fig. 7 shows PXRD diffraction patterns of Ti-TiO_2-OHAp and Ti-TiO_2-OHAp-CaDDP films. It is evident that the phosphate ester surfactant forms a CaDDP lamellar phase, with interlayer *d*-spacings of 36 and 30 Å under the experimental conditions, and that its presence does not adversely affect the OHAp mineral phase. The two different interlayer *d*-spacings probably correspond to distinct degrees of interdigitation or tilting of the hydrophobic tails of the surfactant in the calcium phosphate bilayer. The intensity of the characteristic peaks of hydroxyapatite did not decrease upon formation of the CaDDP which implies that no dissolution occurred during the film growth process.

A SEM micrograph of the calcium dodecylphosphate-hydroxyapatite (CaDDP-OHAp) sample after one day aging time is shown in Fig. 8. It can be seen that the CaDDP phase is coating the film of porous oriented hydroxyapatite crystals and that it is effectively following the contour surfaces of the crystals. The thickness of the CaDDP lamellar phase varies from *ca.* 1–5 μm.

Fig. 9 displays a TEM micrograph of the same sample. It can be seen that the surface of the growing CaDDP lamellar phase is oriented parallel to the OHAp mineral long *c*-axes and moreover is organized in close contact with the crystals. This micrograph is representative of the sample as a whole. It should be noted that the same type of co-assembly phenomenon was observed previously with powdered forms of the CaDDP-OHAp composite material.[15] The authors of this earlier work proposed a model which could rationalize the formation and preferred orientation of the composite material. The model assumed stereochemical, geometrical and charge complementarity between the calcium and phosphate ester sites in the surface region of the CaDDP lamellar phase and calcium and phosphate sites in the [001] face of the hydroxyapatite crystal lattice, with some degree of protonation of the interfacial phosphate groups. Since hydroxyapatite formed on TiO_2 is a non-stoichiometric HPO_4^{2-} containing phase, it is expected that some of these HPO_4^{2-} groups will also be located in the surface regions, particularly because the source of the phosphate used is K_2HPO_4 and the pH of the solution was 7.4. This provides credence for the previously proposed model of the CDDP-OHAp chemical composite material.[15] A schematic illustration of the architecture of the CaDDP-

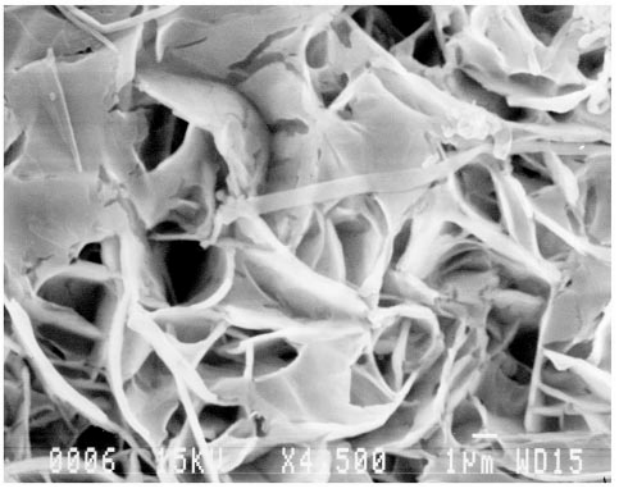

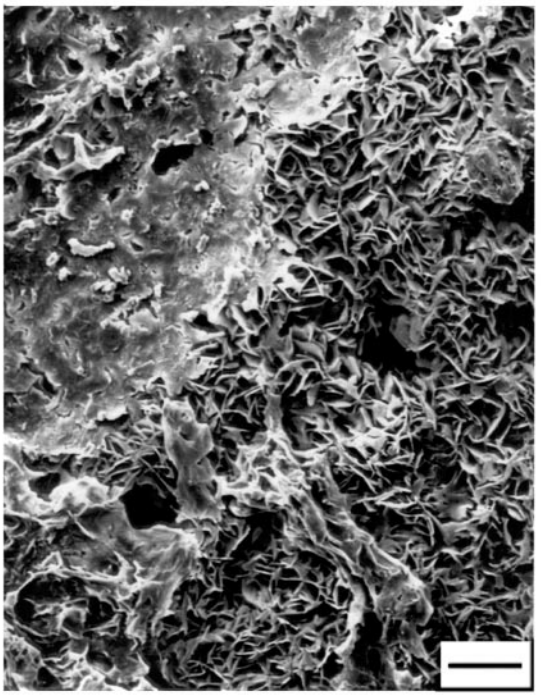

Fig. 8 SEM micrographs that show the deposition of the calcium dodecylphosphate lamellar phase on the surface of the porous oriented hydroxyapatite film. Lamellar phase varies in thickness over the mineral phase; scale bar for the bottom image is 10 μm.

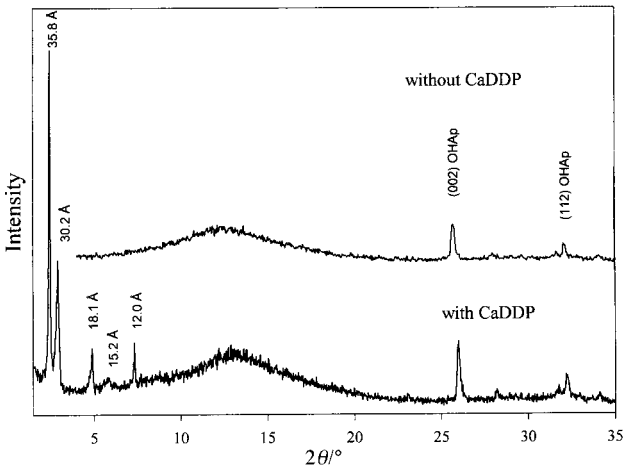

Fig. 7 PXRD diffraction patterns of Ti-TiO_2-OHAp (top) and Ti-TiO_2-OHAp-CaDDP (bottom). The integrity and orientation of the OHAp film is maintained upon deposition of the CaDDP lamellar phase.

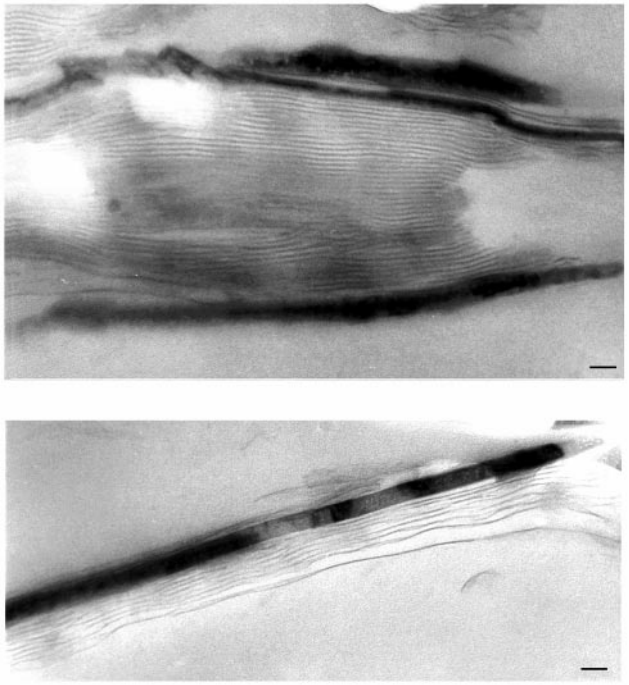

Fig. 9 Cross-sectional TEM micrographs of the calcium dodecylphosphate–hydroxyapatite composite scraped from the titania substrate; scale bar for both images is 45 nm. Particularly interesting is the co-alignment of the long *c*-axis of the OHAp crystals with the (100) plane of the CaDDP suggesting interfacial complementarity between the two.

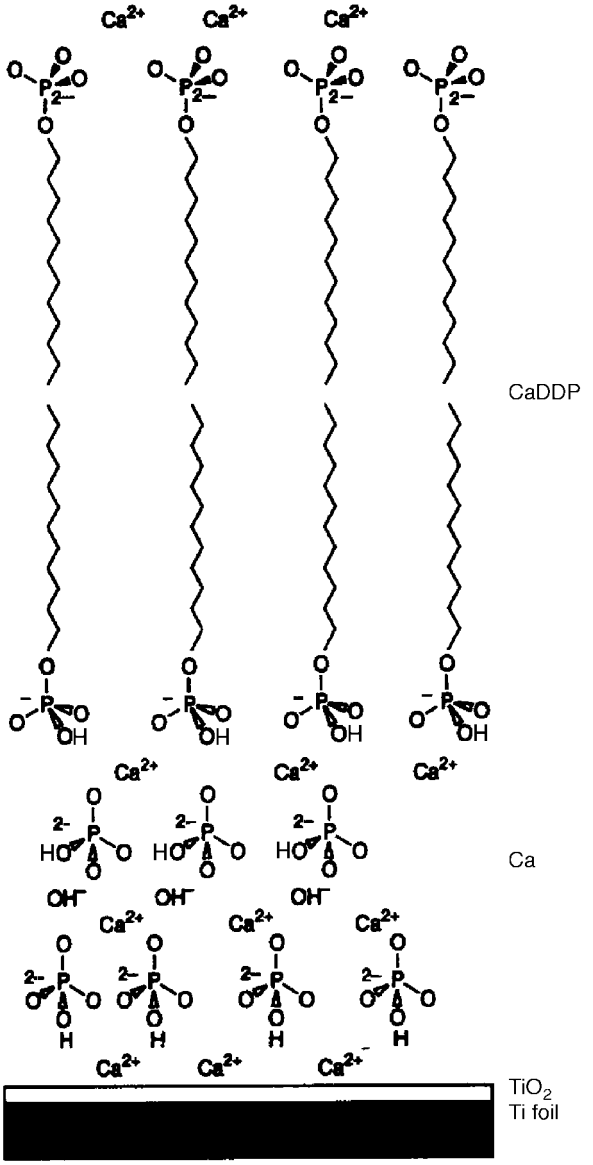

Fig. 10 Illustration of proposed architecture of the CaDDP-OHAp-TiO_2-Ti chemical composite material. Based on the experimental evidence, there exists geometrical and charge matching between Ca^{2+} and $HPO_4^{1-/2-}$ at the interfaces between TiO_2-OHAp and OHAp-CaDDP.

OHAp-TiO_2-Ti composite film established in this study is shown in Fig. 10.

Fig. 11 shows a series of ^{31}P CP MAS NMR results that re-enforces the proposed structural model and interfacial complementarity of the organic–inorganic hierarchical composite material. The ^{31}P MAS NMR spectrum of the organic phase CaDDP shows a single resonance at $\delta -1.4$ and is not enhanced by the cross-polarization technique, Fig. 11(a), consistent with the absence of protons on phosphate groups. The inorganic phase scraped from the TiO_2 substrate exhibits a ^{31}P MAS NMR signal at δ 1.9 with a small broad shoulder at δ *ca.* -1.2. The upfield signal is greatly enhanced by CP, Fig. 11(b), and can be reasonably assigned to protonated phosphate groups present in the sample.[27,28] This is not surprising since the sample comprises highly non-stoichiometric OHAp and OCP. Fig. 11(c) shows the ^{31}P CP MAS NMR spectrum of a physical mixture of the CaDDP phase and scraped-off inorganic hydroxyapatite phase that shows a superposition of peaks from the individual components. The intensity of the signal from the organic phase is enhanced with respect to the inorganic phase, probably due to the contribution from non-directly attached α-methylene protons. It is evident that no additional signals are present implying the environment of phosphorus nuclei remains the same upon physically mixing the two phases. By contrast, at least two new signals appear in the case of the chemical composite material, CaDDP-OHAp scraped from the TiO_2 surface, Fig. 11(d). The CaDDP region shows a new upfield shifted signal at $\delta -4.8$ that could arise from protonation of the phosphate group and/or a change in the O–P–O bond angle.[15,29] Our model, Fig. 10, assumes protonation at the interface but some tilting in the organic phosphate region upon adsorption is likely to occur as well. The inorganic phase exhibits an upfield shift due to protonation at δ 1.1 while shoulders at δ 2.2 and 4.1 could be assigned to the presence of HPO_4^{2-} groups in an OCP environment in the sample.[16] It is clear that the spectrum of the chemical composite is different from that of the physical mixture. The additional ^{31}P signals most likely arise from interfacial interactions involving protonated phosphate sites in the OHAp and CaDDP phases. Similar additional upfield shifted signals were observed in powdered samples[15] and were ascribed to interfacial protonation of phosphate groups.

Conclusion

Fast growth of thick oriented hydroxyapatite crystalline films on a TiO_2 surface occurs as a consequence of precursor OCP nucleation on distinct activation sites of the substrate and *in situ* hydrolysis to the more thermodynamically stable OHAp phase. Porosity, non-stoichiometry and the rate of the OHAp film formation under physiological conditions on the sputter deposited TiO_2 surface render this material as a viable coating for bone implant materials. The presence of HPO_4^{2-} groups are found to be crucial not only with respect to ensuring chemical compatibility with the bone mineral phase but also as a key component for facilitating the formation of an inorganic–organic composite material. The synthesis protocol of growing the OHAp and CaDDP phases sequentially, provides a high level of control over the thickness and composition

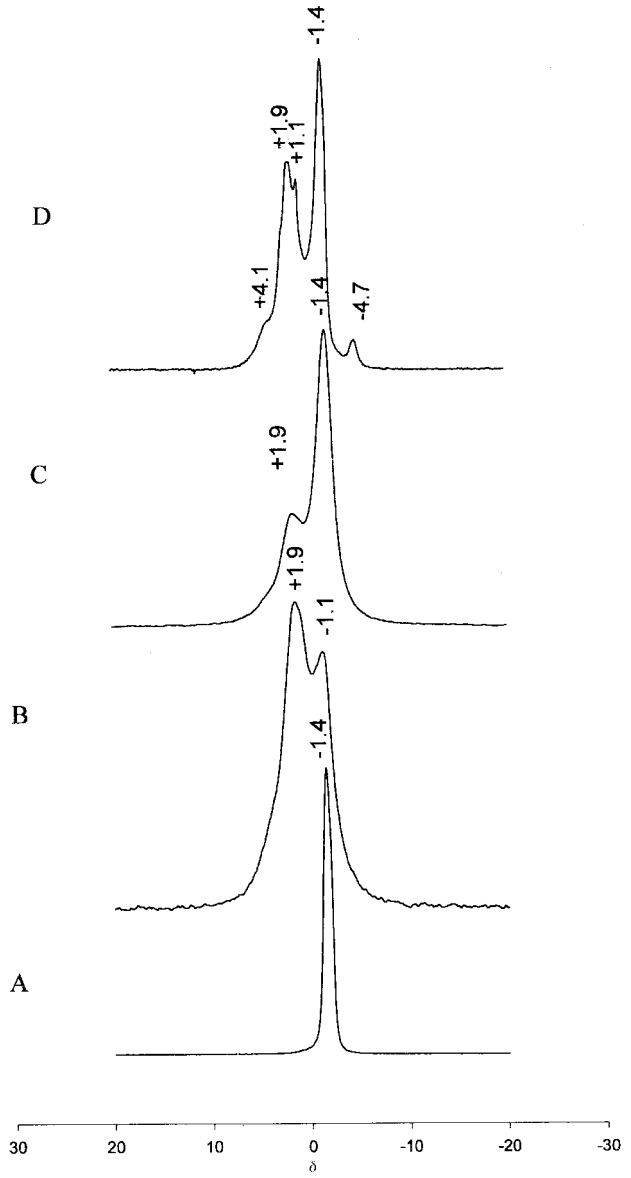

Fig. 11 ^{31}P CP MAS NMR spectra of (a) CaDDP phase (b) hydroxyapatite (c) physical mixture of CaDDP and OHAp (d) chemical composite CaDDP-OHAp. The results show that the chemically formed composite is distinct from a mixture of the components.

of each phase. It also allows for alternation of these phases in a multilayer composite construction, as well as a means for incorporation/release of bioactive substances from the hydrophobic region of the CaDDP lamellar phase, that could improve the response of this type of material in a body environment.

Acknowledgments

G.A.O. is indebted to the Canada Council for the award of an Issac Walton Killam Foundation Research Fellowship, 1995–97. This work was generously funded by the Interdisciplinary Section of the Collaborative Research Program of the Natural Sciences and Engineering Research Council of Canada, NSERC. University of Toronto principal investigators of the project 'Calcium Phosphate Composite Mesostructures as Bone Analogue Materials' are: Dr John E. Davies, Dr Geoffrey A. Ozin, Dr Peter M. Macdonald and Dr Douglas D. Perovic. I.S. is deeply appreciative for the University of Toronto and Gallop memorial scholarships. We are most grateful for technical assistance and stimulating discussions with Dr Neil Coombs, Dr Douglas D. Perovic, Dr Aleksandra Perovic and Dr John Davies with various aspects of the electron microscopy and electron diffraction studies, as well as the bone biology relevant to this inorganic materials chemistry approach to the bone implant problem. The advice of Dr Srebri Petrov with the powder X-ray diffraction measurements is also gratefully acknowledged. The technical assistance and advice of Dr Ömer Dag with FTIR microscopy and optical profilometry, Dr Deepa Khushalani with NMR spectroscopy and Mrs Sue Mamiche-Afara with sputtering is deeply appreciated. The direction of Dr Natasha Varaksa in the early stages of this project proved to be extremely helpful.

References

1 J. Vincent, in *Structural Biomaterials*, Princeton University Press: Princeton, 1990.
2 R. Z. LeGeros, G. Daculsi, I. Orly, T. Abergas and W. Torres, *Scanning Microsc.*, 1989, **3**, 129.
3 D. N. Misra, in *Adsorption on and Surface Chemistry of Hydroxyapatite*, ed. W. E. Brown, M. Mathew and L. C. Chow, Plenum Press, New York, 1984, p. 13.
4 J. C. Elliot, in *Structure and Chemistry of the Apatites and Other Calcium Orthophosphates*, Elsevier, New York, 1994.
5 A. A. Campbell and G. E. Fryxell, J. C. Linehan and G. L. Graff, *J. Biomed. Mater. Res.*, 1996, **32**, 111.
6 W. R. Lacefield, in *Bioceramics: Material Characterizations Versus In Vivo Behavior*; *Ann. New York Acad. Sci.*, eds. P. Ducheyne and J. E. Lemons, 1988, **523**, 72.
7 T. Kokubo, F. Miyaji and H. Kim, *J. Am. Ceram. Soc.*, 1996, **79**, 1127.
8 F. H. Silver, in *Biomaterials, Medical Devices and Tissue Engineering*, Chapman and Hall, New York, 1994.
9 T. Kokubo, *Biomaterials*, 1991, **12**, 155.
10 P. Ducheyne and D. Christiansen, in *Bioceramics 6*, Butterworth-Heinemann, Oxford, 1993.
11 R. Van Noort, *J. Mater. Sci.*, 1987, **22**, 3801.
12 K. de Groot, R. G. T. Geesink, C. P. A. T. Klein and P. Serekian, *J. Biomed. Mater. Res.*, 1987, **21**, 1375.
13 T. Hanawa and M. Ota, *Biomaterials*, 1991, **12**, 767.
14 P. Ducheyne, L. L. Hench, A. Kagan, M. Martens, A. Burssens and J. C. Mulier, *J. Biomed. Mater. Res.*, 1980, **14**, 225.
15 G. A. Ozin, N. Varaksa, N. Coombs, J. E. Davies, D. Perovic and M. Ziliox, *J. Mater. Chem.*, 1997, **7**, 1601.
16 C. Elliot, in *Structure and Chemistry of the Apatites and Other Calcium Orthophosphates*, Elsevier, New York, 1994.
17 C. Rey, M. Shimizu, B. Collins and M. J. Glimcher, *Calcif. Tissue Int.*, 1990, **46**, 384.
18 C. Rey, M. Shimizu, B. Collins and M. J. Glimcher, *Calcif. Tissue Int.*, 1991, **49**, 383.
19 S. R. Radin and P. Ducheyne, *J. Biomed. Mater. Res.*, 1993, **27**, 35.
20 N. Pleshko, A. Boskey and R. Mendelsohn, *Biophys. J.*, 1991, **60**, 786.
21 B. O. Fowler, M. Markovic and W. E. Brown, *Chem. Mater.*, 1993, **5**, 1417.
22 E. L. Bullock, L. Patthey and S. G. Steinemann, *Surf. Sci.*, 1996, **352–354**, 504.
23 T. K. Sham and M. S. Lazarus, *Chem. Phys. Lett.*, 1979, **68**, 426.
24 P. W. Brown and B. Constantz, *Hydroxyapatite and Related Materials*, CRC, Boca Raton, FL, 1994.
25 S. Sugiyama, T. Minami, T. Moriga, H. Hayashi, K. Koto, M. Tanaka and J. B. Moffat, *J. Mater. Chem.*, 1996, **6**, 459.
26 J. L. Ong, L. C. Lucas, G. N. Raikar, J. J. Weimar and J. C. Gregory, *Colloids Surf. A: Physicochem. Eng. Asp.*, 1994, **87**, 151.
27 W. P. Rothwell, J. S. Waugh and J. P. Yesinowski, *J. Am. Chem. Soc.*, 1980, **102**, 2637.
28 M. M. Crutchfield, C. F. Callis, R. R. Irani and G. C. Roth, *Inorg. Chem.*, 1962, **4**, 813.
29 D. G. Gorenstein, *J. Am. Chem. Soc.*, 1975, **97**, 898.

Paper 8/06045B